XXI IMEKO World Congress "Measurement in Research and Industry"
August 30 – September 4, 2015, Prague, Czech Republic

A METHOD OF SELF-TESTING OF ANALOG CIRCUITS BASED ON FULLY DIFFERENTIAL OP-AMPS WITH THE TCBF CLASSIFIER

Zbigniew Czaja [1], *Michał Kowalewski* [2]

[1] Faculty of Electronics, Telecommunications and Informatics, Gdansk University of Technology, Gdansk, Poland, zbczaja@pg.gda.pl
[2] Faculty of Electronics, Telecommunications and Informatics, Gdansk University of Technology, Gdansk, Poland, mickowal@pg.gda.pl

Abstract – A new approach of self-testing of analog circuits based on fully differential op-amps of mixed-signal systems controlled by microcontrollers is presented. It consists of a measurement procedure and a fault diagnosis procedure. We measure voltage samples of a time response of a tested circuit on a stimulation of a unit step function given at the common-mode reference voltage input of the op-amp. The fault detection and fault localization is carried out by the TCBF neural network classifier.

Keywords: neural classifiers, self-testing, microcontrollers, fully differential op-amps.

1. INTRODUCTION

At present, more and more sensors are made in the form of smart sensors which allow to create wired or wireless telemetric networks. The main component of these circuits, more precisely mixed-signal systems, is a control unit which controls measurements, processes measurement data, stores the data and maintains communication among other smart sensors in the network. This unit is built mostly based on microcontrollers and signal processors.

The measurement, that is acquiring information about the sensors environment, as well as about the controlled objects, in many cases is realized using analog sensors – the circuits with analog outputs. Analog signals coming from the analog sensors, prior to their digitalization, are conditioned in analog circuits (analog parts of these systems) – they are amplified and initially filtered to adapt them to the measurement range of ADCs.

An important parameter of smart sensors is their reliability. We can fulfill this condition by implementing self-testing procedures in these systems. These procedures should deal with not only functional testing a whole system, its software and its digital parts, but also its analog parts - what is the topic of the paper.

In many cases the analog parts are realized based on fully differential operational amplifiers (op-amps) dedicated for energy-efficient data acquisition systems.

Taking into account the architecture of testing systems, three methods of testing analog circuits based on fully differential op-amps are distinguished [1]:

- with the common-mode excitation at the input of the stage,
- with a variation of the common-mode reference voltage,
- with the differential-mode excitation.

The best solution is the second one as was presented in [1,2]. In this case, a testing signal is given at the common-mode reference voltage input V_{ocm}, which controls the output common-mode voltage $V_{oc} = (V_{out+} + V_{out-})/2$. If the tested analog circuit is fault free ("symmetric"), the output signal $V_{out} = V_{out+} - V_{out-} = 0$ independently of the V_{ocm} value. An "asymmetry" of the tested circuit ($V_{out} \neq 0$) means that there is at least - and at the same time the most common - a single soft or hard fault in the circuit. Thus, the measurements of parameters of the signal V_{out} for a sinus stimulation [2] or a square pulse [3] allow for the fault detection and the single soft fault localization in passive components.

An important problem for these fault diagnosis methods is masking faults. It follows from the tolerance dispersion of values of no-faulty components. This problem is solved by the use of a classifier based on a Two-Center Basis Function (TCBF) neural network [4,5]. It is characterised by the application simplicity and its high resistance against the component tolerance.

Hence, we propose a new approach of self-testing of analog circuits based on fully differential op-amps of mixed-signal systems controlled by microcontrollers. This approach consists of a measurement procedure realized by the BIST (Buit-In Self-Tester) modified according to the one proposed in [3] and a diagnosis procedure based on the TCBF neural network classifier.

2. THE MEASUREMENT PROCEDURE

The measurement procedure is based on a fault diagnosis method [3], in which, similarly to the methods described in [6,7], we measure voltage samples of a time response of a tested fully differential circuit to a stimulation, but in the form of a unit step function given at the input V_{ocm}. The unit step is generated after a short circuit of the input V_{ocm} to the ground for the specified duration. The stimulation of the tested circuit and voltage sampling of its response are realized by the BIST configured with internal measurement peripherals of a microcontroller, as shown in Fig. 1.

We should underline the fact that for these methods [3,6,7] the fault dictionary consists of fault signatures which can be illustrated in the form of localization curves placed in

the measurement space. This fact is particularly useful for constructing the TCBF neural network classifiers.

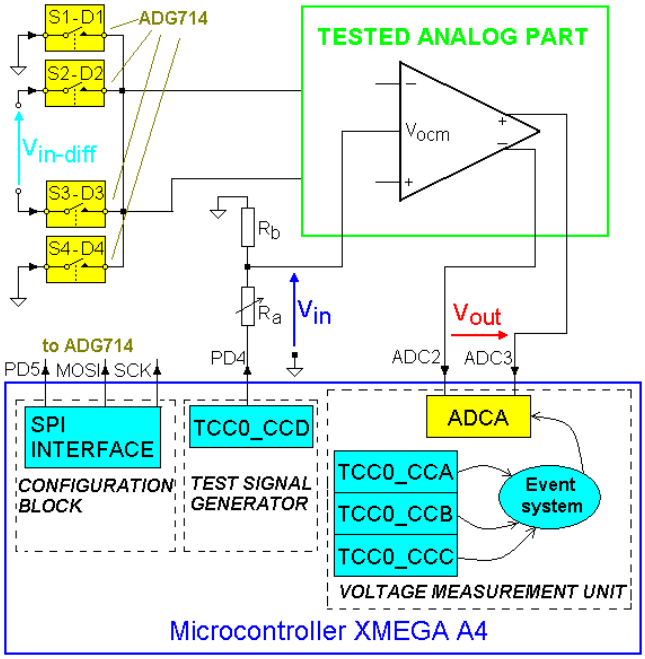

Fig. 1. An example of a mixed-signal system in the self-testing mode of the analog part.

The self-testing of an analog part based on a fully differential op-amp will be presented on an example of the system (Fig. 1) controlled by a 8-bit microcontroller ATXmega32A4 [8]. We use only TC0 (Timer/Counter version 0) for counting the duration of the short circuit of the input V_{ocm} to the ground for discharging all capacitors and determining three voltage sample moments t_1, t_2 and t_3 of the time response of the tested circuit by the ADC A. The TCC0 channels A, B and C (marked on Fig. 1 as TCC0_CCA, TCC0_CCB and TCC0_CCC, respectively) are used to determine triggering the ADC, whereas the channel D (TCC0_CCD) - to determine the discharging signal duration t_0 at the PD4 output. Two ADC channels CH0 and CH1 connected to one common input ADC 2 are used for voltage sampling. The synchronization signals coming from the TC0 via the event system directly trigger the AD conversions. Thanks to the use of the event system, we simplify the algorithm of the measurement procedure and also eliminate the problem of program delays.

A novelty presented in the paper is an extension of the BIST proposed in [3] onto a set of analog switches placed at the inputs and outputs of the tested circuit to enable a change between the normal and self-testing modes of the analog part, and also using an output pin of the microcontroller as the reference voltage applied on a resistive divider R_a, R_b.

For example, in the first case we use the ADG714 [9] containing octal SPST switches controlled by the SPI interface. The use of the ADG714 does not influence a deterioration of the system functionality, because this circuit can be connected together with other circuits equipped with this interface.

In the second case we decided to change the place of a connection of the output pin of the microcontroller to the resistive divider. Thanks to this, we can decide when the reference voltage is turned on, what allows to reduce the energy consumption. However, we should use a potentiometer R_a instead of a resistor, to enable manual tuning of the voltage reference value. This inconvenience results from the output pin resistance depending on the output pin sink current [8].

To illustrate the method, a second order low-pass filter with the MFB topology based on a fully differential op-amp was chosen as the tested analog part (Fig. 2), where R_{1A} = R_{1B} = 10 kΩ, R_{2A} = R_{2B} = 10 kΩ, R_{3A} = R_{3B} = 5 kΩ, C_{1A} = C_{1B} = 10 nF, C_2 = 20 nF.

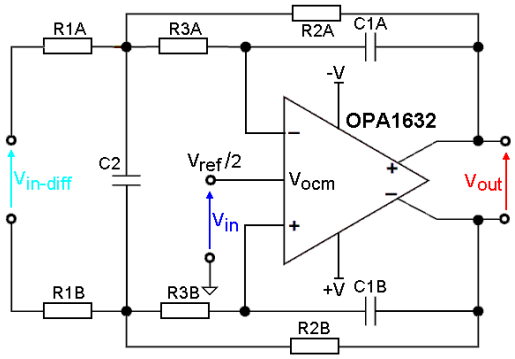

Fig. 2. The tested analog part – a second order low-pass filter with the MFB topology based on a fully differential op-amp.

The timing of the measurement procedure is shown in Fig. 3. After a short circuit of the input V_{ocm} to the ground by the time t_0 needed for discharge all capacitors, that is after the introduction of the tested circuit to the initial state, the purpose measurement procedure is started. At time t = 0 s the constant voltage $V_{ref}/2$ is applied at the input V_{ocm}. When the circuit is fault-free the output differential voltage v_{out} equals to zero, but a single fault results in occurring a signal with its shape being crucial to identify the fault. The response signals $v_{out}(t)$ for single faults of resistors and capacitors are shown in Fig. 3. The following deviations of element values were assumed: $0.1X_{nom}$ (suffix '–' in the fault signature) and $10X_{nom}$ (suffix '+'), where X_{nom} is the nominal value of the element.

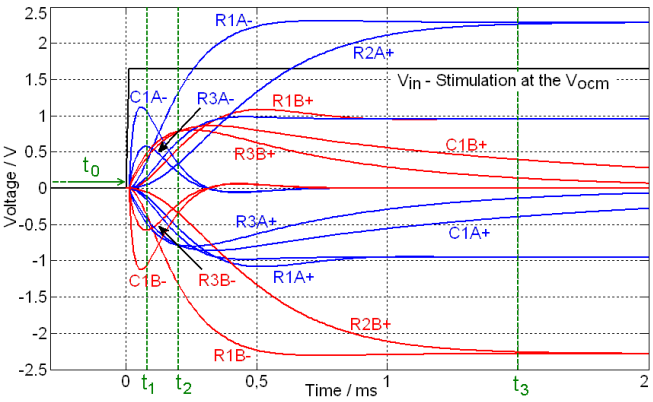

Fig. 3. The timing of the measurement procedure.

The procedure assumes measuring three differential voltage samples at the moments t_1, t_2 and t_3, counting from the start of generating the stimulation by the ADC working in the differential input mode. As a result of the measurement procedure we obtain the measurement point with coordinates ($V_{out}(t_1)$, $V_{out}(t_2)$, $V_{out}(t_3)$). Next, this point is forwarded to the fault diagnosis procedure, which consists first in the fault detection and then the localization of single faults with the use of a neural network classifier with TCB functions.

The algorithm of the measurement procedure is partly implemented in the software (Fig. 4), and partly "built-in" in the configuration of peripheral devices of the microcontroller (Fig. 5). Therefore, it should be noted that the description of the measurement procedure takes into account the simultaneous analysis of these two figures.

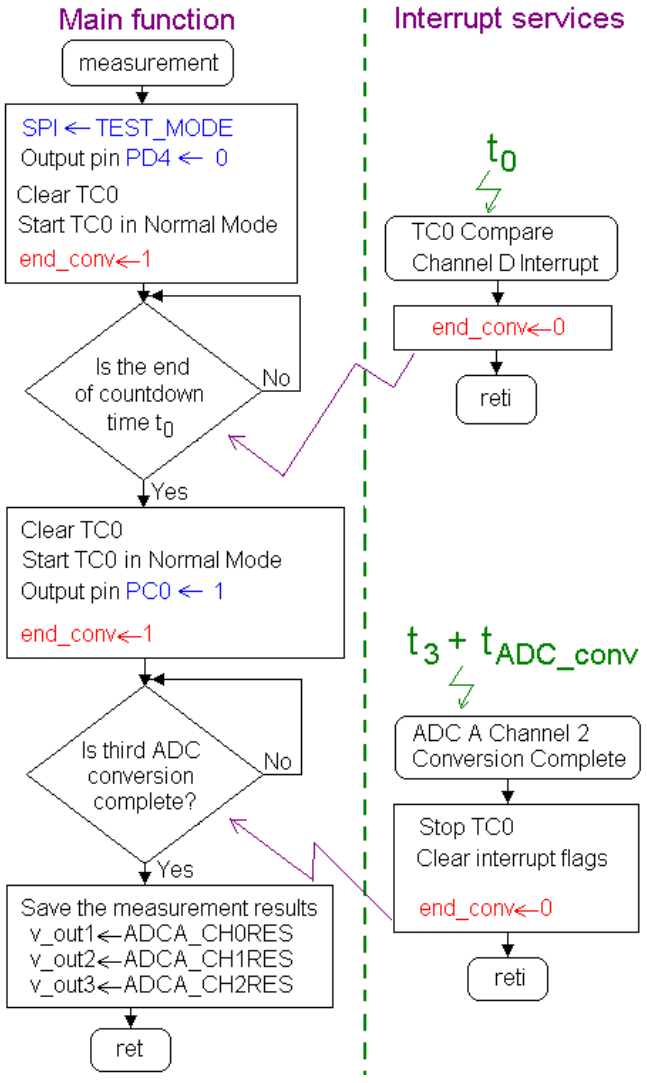

Fig. 4. The flowchart of the algorithm of the measurement procedure.

The software of the measurement procedure consists of three code sections. The code placed in the main body of the measurement function responsible for starting the measurement microsystem, and two codes of the interrupt services for the TC0 and the ADC A (Fig. 4).

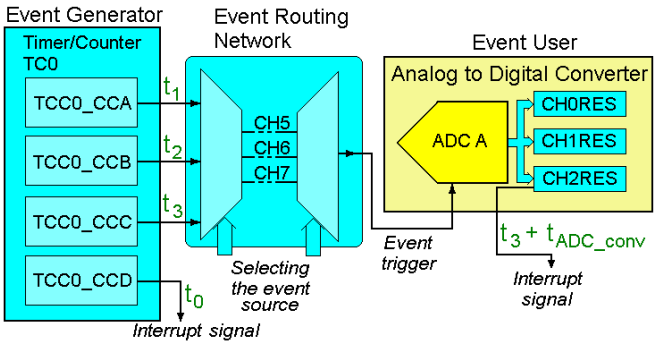

Fig. 5. Block scheme of the measurement microsystem configured from peripherals of the microcontroller ATXmega32A4.

At the beginning of the measurement function we introduce the circuit in the self-testing mode by the change of switch settings of the ADG714 – sending 05h to the ADG714 via the SPI. Next we set V_{in} = 0 V at the pin PD4 to introduce the tested circuit to the initial state. After the time t_0 counted by the TC0, the interrupt is generated. In its service the flag *end_conv* is cleared what causes a transition to the main function code. At this moment we run the purpose measurement procedure. The TC0 is cleared and run in the Normal Mode and a high level at the PC0 pin is set – the beginning of the a unit step function signal at the input V_{ocm}. The match in the TCC0_CCA (counting the time t_1) triggers the first AD conversion on the CH0, the match in the TCC0_CCB (counting the time t_2) triggers the second one on the CH1 and the match in the TCC0_CCC (counting the time t_3) triggers the third one on the CH2. The last AD conversion complete (after the time $t_3 + t_{ADC\_CONV}$, where t_{ADC_CONV} is the AD conversion time of the ADC A [8]) generates the interrupt, in which service the TC0 is stopped, all AD conversion complete interrupt flags are cleared and also the flag *end_conv* is cleared. At the end of the measurement function we save three AD conversion results placed in the ADC A result registers CH0RES, CH1RES, CH2RES to the 16-bit variables v_out1, v_out2, v_out3, adequately.

3. THE FAULT DIAGNOSIS PROCEDURE

Diagnosing of the analog part is realized in two stages.

In the first stage a "go/no-go" test is performed. It depends on comparing the measured samples $V_{out}(t_1)$, $V_{out}(t_2)$ and $V_{out}(t_3)$ with the voltage values ± 10 mV. These voltage limits result from a dispersion of the differential voltage V_{out} following from 1 % tolerances of RC elements. If at least one sample goes beyond the assumed voltage range a fault is present and that fault can be localized in the next stage.

The localization of faults is a second stage of the diagnosis procedure and is performed using the functions of a TCBF neural network classifier. This classifier is able to localize single soft and hard faults as well as to detect multiple faults, when more than one element's value extends ± 1 % of the tolerance range of elements. Only faults of resistors and capacitors were assumed. For the sake of constructing the classifier there is also a possibility to identify faults with a limited degree, but that functionality was omitted in the presented diagnosis procedure.

4. CONSTRUCTION OF THE CLASSIFIER

The basic unit in the classifier is a TCB function, which radially transforms the space around a line segment connecting two points in the measurement space according to the following equation [5]

$$y(\mathbf{x}) = \exp\left(-\frac{1}{2s^2(\mathbf{x})} \left(\mathbf{x} - \mathbf{w}(\mathbf{x})\right)^{\mathrm{T}} \mathbf{C} \left(\mathbf{x} - \mathbf{w}(\mathbf{x})\right) \right), \quad (1)$$

where $\mathbf{x}$ is an input vector, $\mathbf{w}(\mathbf{x})$ is a vector of center functions, $s(\mathbf{x})$ is a scaling function and $\mathbf{C}$ is a scaling matrix describing the TCB function activation region. The TCB function value decreases from 1 to 0 along with increasing the distance between the measurement point and that line segment. A similar situation occurs in the case of a Gauss function used in the hidden layer of Radial Basis (RB) function neural network. However, in contrast to the TCB function, the Gauss function radially transforms the space around a point in the measurement space and its activation range is limited. Exemplary shapes of Gauss and TCB functions for arguments x_1 and x_2 are shown in Fig. 6.

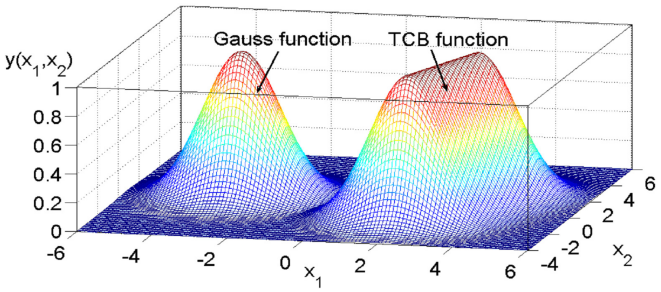

Fig. 6. Activation areas of Gauss and TCB functions.

The performed research with use of both types of basis functions in neural classifiers dedicated to the localization of faults clearly proved advantages of the classifier with TCB functions [4,5]. They result from the fact that elongated shapes of TCB functions allow to better fit neurons to dispersed localization curves, which are used to model parametric faults. There is also a decrease of the number of neurons in the hidden layer relating to the radial neural network with Gauss functions, which is well known and used in diagnosis applications.

A classifier with TCB functions was developed. It enables to localize single faults of RC elements in the analog part of a mixed-signal system. The classifier can be realized in the form of an algorithm in the source code of a microcontroller.

The architecture of the TCB function classifier is presented in Fig. 7. The classifier has two layers of neurons. TCB functions are placed in the hidden layer and are assigned to localization curves. Each localization curve is connected with variations of one element (either R or C) value in the analog part.

A measurement vector $\mathbf{x}$ applied to each TCB function is composed of three voltage samples $V_{out}(t_1)$, $V_{out}(t_2)$ and $V_{out}(t_3)$ acquired in the measurement procedure. The output values of neurons with TCB functions are arguments to neurons in the output layer, which assign TCB functions to the localization curves. These neurons are marked as M_1, M_2, …, M_k, …, M_K. The neuron M_k produces maximum values of all TCB function outputs assigned to the localization curve k and its functionality can be interpreted as an extension of activation regions of individual TCB functions. The element y_k in the output vector $\mathbf{y} = [y_1, \ldots, y_K]$ gives an information about the distance in the n-dimensional space between the measurement point $\mathbf{x} = [V_{out}(t_1), V_{out}(t_2), V_{out}(t_3)]$ and the localization curve k. This information is given as a value within the range (0, 1]. If the point $\mathbf{x}$ is placed near the localization curve k then the value of y_k is close to 1. The value y_k decreases to 0, if the point $\mathbf{x}$ is distant from the curve k.

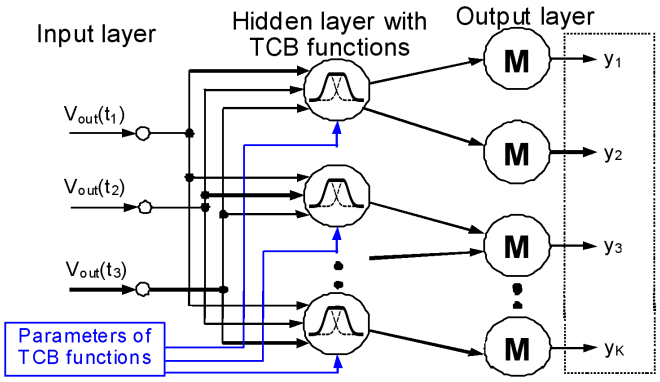

Fig. 7. The architecture of the TCB function classifier.

The information about the state of the object under test can be obtained by analysing values in the output vector $\mathbf{y}$ of the classifier, as was described in [4]. The TCB function classifier is able to localize single faults and detect multiple faults. In the first case the highest value in the output vector $\mathbf{y}$ indicates the faulty component. In the second case all M_k values are close to zero, which means that the measurement point is far from all localization curves.

An important factor in the proper operation of the classifier is selecting optimal values of its parameters (coordinates of centers, scaling parameters and matrices). These parameters depend on the tested analog part topology and the values of its elements. They are obtained in the before-test stage on the basis of the analog part model simulation. This process is realized in two stages described in following subsections.

4.1. Evaluation of coordinates of centers

In the first stage coordinates of centers of TCB functions are calculated on the basis of the analog part tolerance-free model simulation. For each element X a set of values is selected in the range from $0.1X_{nom}$ to $10X_{nom}$ and nominal localization curve is evaluated. Then localization curve is divided into two sections corresponding to values lower or greater than the nominal value X_{nom}. For each section of the localization curve an interpolation curve composed of connected line segments, with endpoints localized on the localization curve, is evaluated. Starting from two points in the measurement space obtained for extreme values of the

element in next iterations new points are added for which distance between localization and interpolation curves is the greatest. Iterations are repeated until maximum distance between these curves is greater than assumed maximum distance d_{max}. A set of points $\mathbf{c}^{(k)}$ (k = 1, ..., n_w) obtained for each section is used as centers of n_w – 1 TCB functions, in particular centers $\mathbf{c}^{(j)}$ and $\mathbf{c}^{(j+1)}$ (j = 1, ..., n_w – 1) are assigned to j TCB function. The method of TCB functions centers selection for exemplary localization curve in the 2-dimensional measurement space with coordinates x_1 and x_2 is illustrated in Fig. 8.

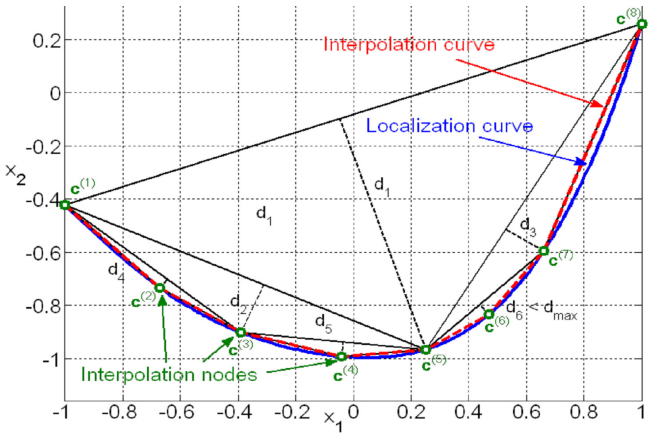

Fig. 8. Steps of determination of exemplary interpolation curve.

In a presented example after 6 iterations an interpolation curve with 8 points (n_w – 8) was obtained. Coordinates of this points are used as centers of 7 TCB functions.

4.2. Evaluation of scaling parameters and matrices

In the second step dispersed localization curves are constructed for 1 % tolerances of elements. The statistical analysis of the dispersed localization curves enables to obtain scaling parameters and matrices of TCB functions.

Determining degree of dispersion of localization curves is focused only on interpolation nodes, which are used as centers of TCB functions. With assumption of identical tolerances of RC elements, for deviation k of a parameter X with respect to the nominal value X_{nom} one obtains a cluster C_k. A signature of a fault in the cluster C_k is assumed to be a n-dimensional random variable subjected to multivariate normal distribution. With that assumption a scaling matrix $\mathbf{C}$ of the TCB function is an inverse of a covariance matrix $\mathbf{\Sigma}$ of the cluster C_k.

As results from (1) the scaling matrix $\mathbf{C}$ can simultaneously describe shape and width of the TCB function. Due to changeable degree of dispersion along the localization curve it is desirable to introduce a normalized scaling matrix. In that case, width of the TCB function can be controlled only with parameters σ_1 and σ_2 of two concentration ellipsoids f_1 and f_2 created for clusters C_1 and C_2 in the neighborhood of centers $\mathbf{c}^{(1)}$ and $\mathbf{c}^{(2)}$ located in the next interpolation nodes. For that purpose radiuses of all concentration ellipsoids of the classifier are normalized to ones and values of parameters σ_1 and σ_2 are evaluated from a covariance matrix $\mathbf{\Sigma}$, according to the formula

$$\sigma_i = \sqrt{F^{-1}(P, n)}, \quad i = 1, 2, \tag{2}$$

where F^{-1} is an inverted cumulative distribution of a parameter σ, which has distribution χ^2, n is a dimension of space and P = 0,9973 is a probability corresponding to confidence interval ± 3 σ for n = 1.

Important decrease of occupancy of the memory by parameters of the classifier can be realized with reference to method of storage scaling matrices of TCB functions. These matrices are evaluated on the basis of covariance matrices, which are symmetrical. Hence, it is preferably to store only coefficients of upper or lower triangular matrices.

In the diagnosis procedure a method with upper triangular matrices was used. In order to decrease computational complexity of the TCB function, an algorithm of calculating functional $\mathbf{x}^T\mathbf{A}\mathbf{y}$ was developed (Fig. 9).

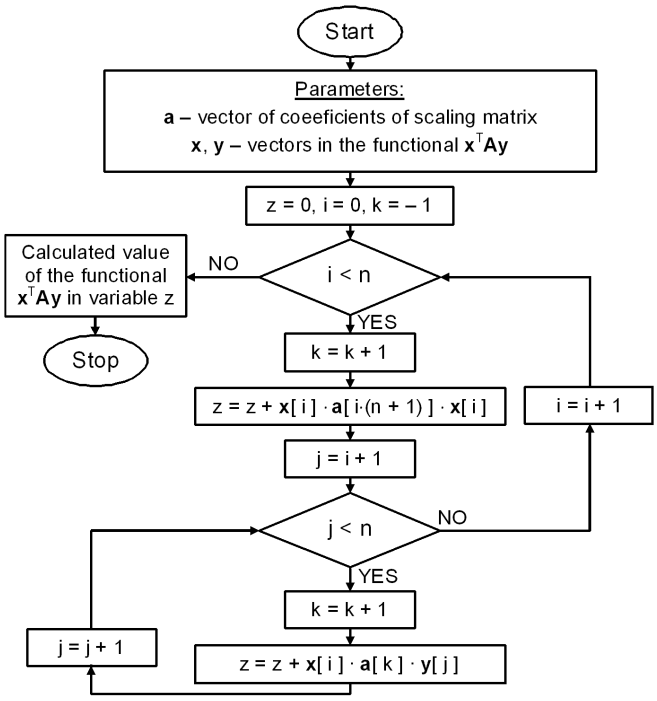

Fig. 9. The algorithm of calculating functional $\mathbf{x}^T\mathbf{A}\mathbf{y}$.

Parameters of the algorithm are vectors $\mathbf{x} = [x_1, ..., x_n]^T$, $\mathbf{y} = [y^1, ..., y_n]^T$ and vector $\mathbf{a}$ containing coefficients of the scaling matrix $\mathbf{C}$, e.g. in case of the 3-dimensional upper triangular matrix, coefficients of vector $\mathbf{a}$ are as follows:

$$\mathbf{a} = [a_{11}, a_{12}, a_{13}, a_{22}, a_{23}, a_{33}]. \tag{3}$$

Decrease of memory demands followed from storing only coefficients of upper triangular scaling matrices for 3-dimensional space equals 33 %.

5. IMPLEMENTATION OF THE CLASSIFIER

The TCB function classifier can be used for the fault localization in the analog part presented in Fig. 2. Parametric faults of RC elements in the range from $0.1X_{nom}$ to $10X_{nom}$ (X = R, C) are considered. A few hundred simulations should

be performed, which depend on applying the constant voltage $V_{ref}/2$ at the input V_{ocm} at the moment $t = 0$, acquiring differential voltage samples V_{out} at the moments $t_1 = 0{,}08$ ms, $t_2 = 0{,}2$ ms and $t_3 = 1{,}5$ ms and plotting the localization curves in the three-dimensional input space with the coordinates ($V_{out}(t_1)$, $V_{out}(t_2)$, $V_{out}(t_3)$) (Fig. 8). Sampling moments are selected with use of a method maximizing distances between the fault signatures in the measurement space.

In the next step the centers of TCB functions are selected. For that purpose a method based on a linear interpolation of localization curves with line segments should be used. For the considered analog part a set of 39 centers was obtained, which was used for constructing the classifier with 38 TCB functions. The selected centers of TCB functions are marked in Fig. 10 as black circles. Some faults are equivalent, hence the following groups of equivalent faults must be considered: {R_{1A}–, R_{1B}+, R_{2B}–}, {R_{1A}+, R_{1B}–, R_{2A}–}, {R_{3A}+, C_{1A}+}, {R_{3B}+, C_{1B}+}.

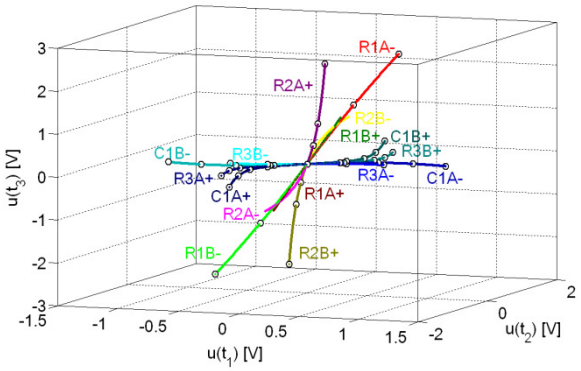

Fig. 10. The family of localization curves for the tested analog part with marked centers of TCB functions.

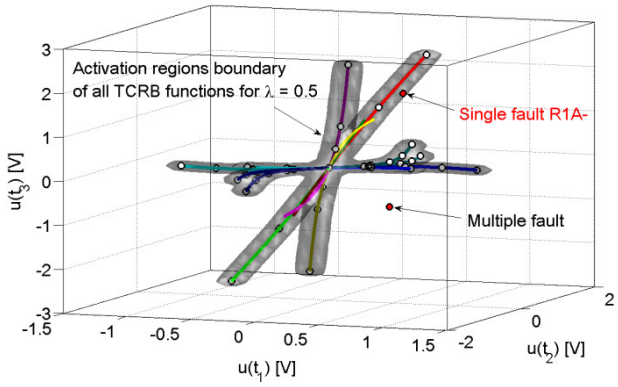

Fig. 11. Activation regions of TCB functions of the classifier.

The last but one step of implementing the classifier depends on selecting the scaling parameters of TCB functions. For that purpose 1 % tolerances of RC elements can be assumed and Monte Carlo simulations must be performed. For the sake of small differences in dispersion of signatures around centers, a constant value of the scaling parameter for all TCB functions can be selected. It allows a significant simplification of the calculation algorithm. Activation regions of all TCB functions of the classifier are shown in Fig. 11. The marked red points indicate exemplary measurement points for a single fault of the element R_{1A} and for a multiple fault. In order to distinguish between a single fault and a multiple fault one needs to compare the output values $y_1, \ldots, y_K$ of the classifier with the threshold level λ ($0 < \lambda < 1$). For a single fault of the element R_{1A} only one value y_k ($k = 1, \ldots, k, \ldots, K$) is greater than λ. For a multiple fault all y_k values are lower than λ.

The last step of the classifier implementation depends on coding parameters of the classifier in the form of fixed-point values and writing them along with the classifier algorithm in the microcontroller memory.

6. CONCLUSIONS

The method of self-testing of analog parts of mixed signal systems is dedicated to diagnosing circuits with fully differential operational amplifiers. The excitation signal in the form of a unit step function is applied at the input V_{ocm}. The diagnosis is performed in the following steps: the detection of a fault, the localization of single faults and the detection of a multiple fault. The last two steps are performed with use of the TCB function neural classifier. The computational complexity of the classifier is not big and its parameters are evaluated in the before-test stage, hence there is a possibility to implement the proposed method even on a simple 8-bit microcontroller.

REFERENCES

[1] W. Toczek, "Self-testing of fully differential multistage circuits using commonmode excitation", *Microelectronic Reliability*, vol. 48, pp. 1890–1899, 2008.

[2] W. Toczek, Z. Czaja, "Diagnosis of fully differential circuits based on a fault dictionary implemented in the microcontroller systems", *Microelectronics Reliability*, vol. issue 8, pp. 1413-1421, 2011.

[3] Z. Czaja, „Self-testing of an analog part based on fully differential op-amps in electronic embedded systems controlled by microcontrollers", "Samotestowanie toru analogowego ze wzmacniaczem w pełni różnicowym w elektronicznych systemach wbudowanych sterowanych mikrokontrolerami", *Pomiary Automatyka Kontrola*, vol. 60, pp. 368-371, 9/2014.

[4] Z. Czaja, M. Kowalewski, "An Application of TCRBF Neural Network in Multi-node Fault Diagnosis Method", *XIX IMEKO World Congress*, pp. 503-508, Lisbon, Portugal, Sept. 2009.

[5] Z. Czaja, M. Kowalewski, "Usage of two-center basis function neural classifiers in compact smart resistive sensors, *XX IMEKO World Congress,* Busan, Korea, 6 pages, Sept. 2012,

[6] Z. Czaja, "A diagnosis method of analog parts of mixed-signal systems controlled by microcontrollers", *Measurement*, vol. 40, issue 2, pp. 158-170, 2007.

[7] Z. Czaja, "Self-testing of analog parts terminated by ADCs based on multiple sampling of time responses", *IEEE Transaction on Instrumentation and Measurement*, vol. 62, issue 12, pp. 3160-3167, 2013.

[8] Atmel Corporation, "Atmel AVR XMEGA AU Manual", online: www.atmel.com., 12/2012.

[9] Analog Devices Inc., "CMOS, Low Voltage Serially Controlled, Octal SPST Switches ADG714/ADG715", online: www.analog.com, 2002.